Structure, Vol. 12, 1683–1691, September, 2004, ©2004 Elsevier Ltd. All rights reserved. DOI 10.1016/j.str.2004.07.009

Crystal Structure of the Carboxyltransferase Domain of Acetyl-Coenzyme A Carboxylase in Complex with CP-640186

Hailong Zhang, Benjamin Tweel, Jiang Li, and Liang Tong*
Department of Biological Sciences
Columbia University
New York, New York 10027

Summary

Acetyl-coenzyme A carboxylases (ACCs) are important targets for the development of therapeutic agents against obesity, diabetes, and other diseases. CP-640186 is a potent inhibitor of mammalian ACCs and can reduce body weight and improve insulin sensitivity in test animals. It is believed to target the carboxyltransferase (CT) domain of these enzymes. Here we report the crystal structure of the yeast CT domain in complex with CP-640186. The inhibitor is bound in the active site at the interface of a dimer of the CT domain. CP-640186 has tight interactions with the putative biotin binding site in the CT domain and demonstrates a distinct mode of inhibiting the CT activity as compared to the herbicides that inhibit plant ACCs. The affinity of inhibitors for the CT domain has been assessed using kinetic and fluorescence anisotropy binding studies. The structural information identifies three regions for drug binding in the active site of CT.

Introduction

Obesity is a serious health problem in both the developed and developing countries (Hill et al., 2003). In the US, 30% of the population are obese, while another 35% are overweight. Moreover, being obese significantly increases the risk for other diseases, especially type 2 diabetes and cardiovascular diseases. There is an urgent need for behavioral changes (food intake and physical activities) in the general population, as well as therapeutic agents to control the spread of this epidemic.

Acetyl-coenzyme A carboxylases (ACCs) are crucial for the metabolism of fatty acids and are promising targets for drug development against obesity, diabetes, and other diseases. ACCs catalyze the conversion of acetyl-CoA to malonyl-CoA (Abu-Elheiga et al., 2001; Alberts and Vagelos, 1972; Cronan and Waldrop, 2002; Wakil et al., 1983). The eukaryotic ACCs are large, multidomain enzymes and contain the biotin carboxylase (BC), biotin carboxyl carrier protein (BCCP), and carboxyltransferase (CT) domains (Figure 1A). The BC domain catalyzes the first step of the reaction, carboxylation of the biotin group that is covalently linked to BCCP, and then the CT domain catalyzes the transfer of this activated carboxyl group to the acetyl-CoA substrate.

Two isoforms of ACCs are present in mammals. ACC1 is a cytosolic enzyme, and it controls the committed step in the biosynthesis of long-chain fatty acids (Wakil et al., 1983). ACC2 is associated with the outer membrane of mitochondria, and its malonyl-CoA product is a potent inhibitor of the transport of long-chain acyl-CoAs for oxidation in the mitochondria (McGarry and Brown, 1997; Ramsay et al., 2001). Mice lacking ACC2 have elevated fatty acid oxidation, reduced body fat and body weight (Abu-Elheiga et al., 2001), indicating the importance of this enzyme for drug discovery (Abu-Elheiga et al., 2003; Lenhard and Gottschalk, 2002).

CP-640186 has recently been shown by researchers at Pfizer Inc. to be a potent inhibitor of both isoforms of mammalian ACCs (Figure 1B), with IC_{50} values of about 55 nM (Harwood et al., 2003). This is currently the only reported potent inhibitor of mammalian ACCs. In cell cultures as well as in animal models, the compound can reduce tissue malonyl-CoA levels, inhibit fatty acid biosynthesis, and stimulate fatty acid oxidation. Most importantly, the compound can reduce body fat mass and body weight, and improve insulin sensitivity, validating ACCs as targets for antiobesity and antidiabetes drugs (Harwood et al., 2003). These observations also suggest that dual inhibitors of both isoforms of mammalian ACCs may be better therapeutic agents than those that solely inhibit ACC2 (Harwood et al., 2003). Kinetic studies show that the compound is noncompetitive versus the acetyl-CoA substrate, but may function at the active site of the CT domain (Harwood et al., 2003).

While CP-640186 targets the mammalian ACCs, potent inhibitors of ACCs from some plants have been widely used as commercial herbicides for more than 30 years (Devine and Shukla, 2000; Gronwald, 1991). These herbicides belong to two different chemical classes, as represented by haloxyfop (FOPs) and sethoxydim (DIMs). They kill sensitive plants by shutting down fatty acid biosynthesis. Mutations of either of two residues (Ile→Leu at one site or Ile→Asn at the other) in the CT domain of plant ACCs can confer resistance to these herbicides (Delye et al., 2003; Jelenska et al., 2002; Zagnitko et al., 2001), suggesting that the compounds may interact with the CT domain of ACC. This is also supported by kinetic data on the inhibition of plant ACCs by these herbicides (Devine and Shukla, 2000; Gronwald, 1991; Rendina et al., 1990).

We recently reported the crystal structures of the free enzyme and CoA complex of yeast CT domain (Zhang et al., 2003), as well as its complex with the herbicides haloxyfop or diclofop (Zhang et al., 2004). The structures reveal that the active site of the CT domain is located at the interface of a dimer of the enzyme. The FOP inhibitors are located in the dimer interface and inhibit the enzyme by disrupting the binding or the conformation of the acetyl-CoA or malonyl-CoA substrate, consistent with our kinetic data demonstrating competitive inhibition of haloxyfop versus malonyl-CoA. The binding of FOPs requires large conformational changes for several residues in the active site of the CT domain, especially Tyr1738 and Phe1956, as well as a change in the organization of the dimer. The two residues that confer resistance to the herbicides when mutated, equivalent to Leu1705 and Val1967 of yeast ACC, are located in

*Correspondence: tong@como.bio.columbia.edu

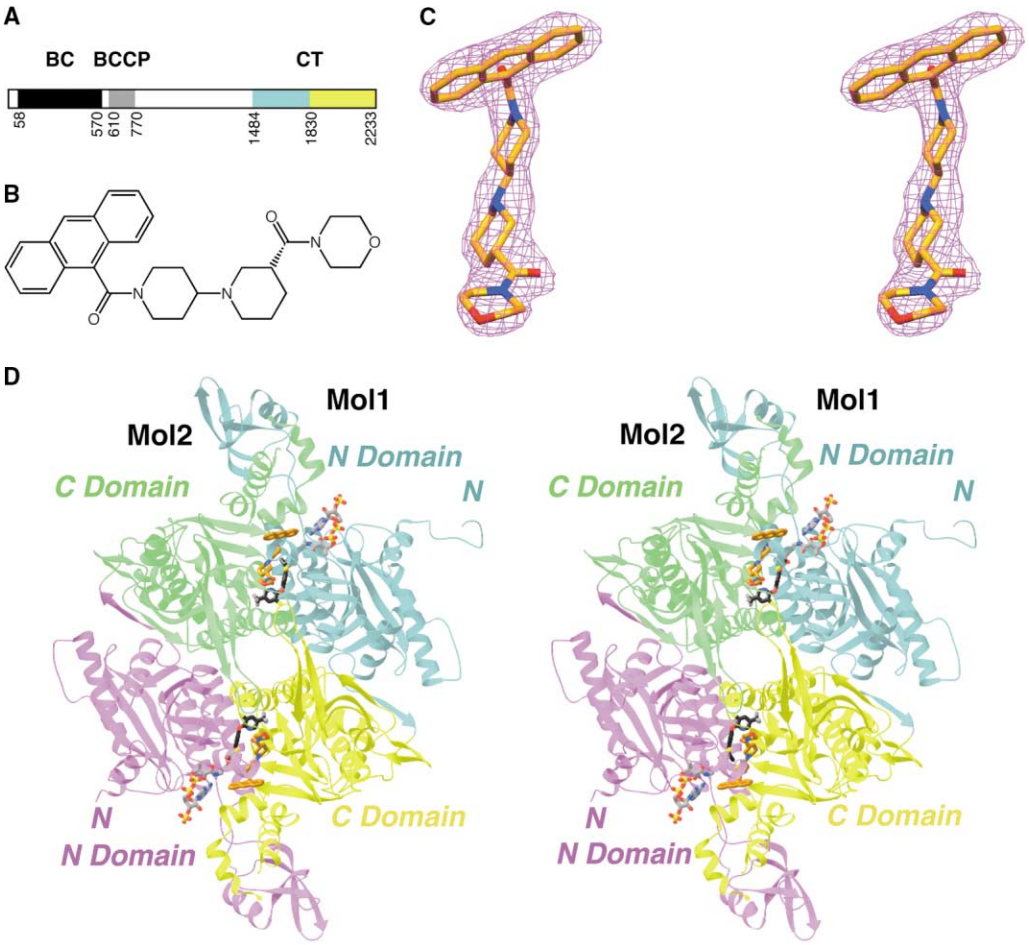

Figure 1. CP-640186 and Its Complex with the CT Domain

(A) Domain organization of eukaryotic ACCs. BC, biotin carboxylase; BCCP, biotin carboxyl carrier protein; CT, carboxyltransferase. The residue numbers are for yeast ACC.

(B) Chemical structure of *R*-CP-640186.

(C) Final omit $2F_o - F_c$ electron density at 2.8 Å resolution for CP-640186, contoured at 1σ.

(D) Schematic drawing of the structures of yeast CT domain dimer in complex with CP-640186 (in gold). The N domains of the two monomers are colored in cyan and magenta, and the C domains are colored in yellow and green. The positions of haloxyfop (black) and CoA (gray) are shown for reference. Panel (C) was produced with SETOR (Evans, 1993) and (D) with Ribbons (Carson, 1987).

the binding site and are the only residues that show variations among the ACCs.

We present here the crystal structure of yeast CT domain in complex with CP-640186 at 2.8 Å resolution. The compound has tight associations with the active site of the enzyme but has a distinct mechanism of inhibiting the CT domain as compared to the FOPs. CP-640186 may block the binding of the biotin substrate to the CT domain, and it requires essentially no conformational change in the CT domain for binding. Our studies identify three regions in the active site of CT that can be targeted for drug binding. We have developed a fluorescence anisotropy binding assay that can measure the affinity of CP-640186 and other inhibitors for the CT domain.

Results and Discussion

The Overall Structure

To reveal the molecular mechanism for the inhibitory action of CP-640186 (Figure 1B), we have determined the crystal structure of the yeast CT domain in complex with this compound at 2.8 Å resolution (Table 1). The complex with CP-640186 was obtained by soaking crystals of the free enzyme with this compound, and the crystallographic analysis showed clearly defined elec-

Table 1. Summary of Crystallographic Information

Resolution range for refinement (Å)	30–2.8
Number of observations	238,996
R_{merge}[a] (%)	5.7 (23.1)
Number of reflections	92,729
Completeness (%)	86 (65)
R factor[b] (%)	19.7 (27.1)
Free R factor[b] (%)	23.4 (30.2)
Rms deviation in bond lengths (Å)	0.007
Rms deviation in bond angles (°)	1.3

The numbers in parentheses are for the highest resolution shell.

[a] $R_{merge} = \sum_h \sum_i |I_{hi} = \langle I_h \rangle| / \sum_h \sum_i I_{hi}$.

[b] $R = \sum_h |F_h^o - F_h^c| / \sum_h F_h^o$

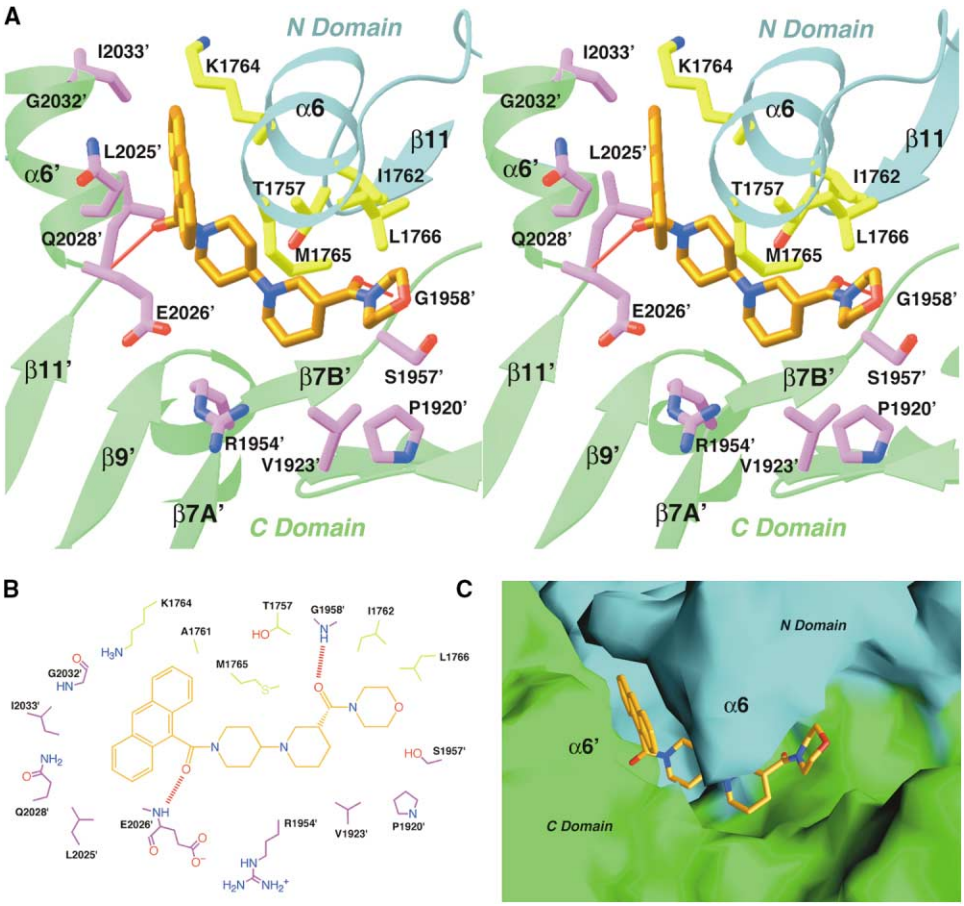

Figure 2. The Binding Mode of CP-640186

(A) Stereographic drawing showing the binding site for CP-640186. The N domain of one monomer is colored in cyan and the C domain of the other monomer in green. The side chains of residues in the binding site are shown in yellow and magenta, respectively. The hydrogen bonds from the inhibitor are shown as thin red lines. This panel was produced with Ribbons (Carson, 1987).

(B) Schematic drawing of the interactions between CP-640186 and the yeast CT domain.

(C) Molecular surface of the binding site for CP-640186 in the yeast CT domain. This panel was produced with Grasp (Nicholls et al., 1991).

tron density for the inhibitor (Figure 1C). The current atomic model has excellent agreement with the observed diffraction data and the expected chemical parameters (Table 1), and 86% of the residues are in the most favored region of the Ramachandran plot (data not shown).

There are three molecules of the CT domain in the crystallographic asymmetric unit, and they have essentially the same conformation. The rms distance between equivalent Cα atoms of any pair of these monomers is 0.4 Å. Two of the monomers form a noncrystallographic dimer (Figure 1D), whereas the third monomer is situated near the crystallographic 2-fold axis and forms a crystallographic dimer. The organization of these two dimers is also similar, with rms distance of 0.4 Å for their equivalent Cα atoms.

The expression construct covers residues 1476–2233 of yeast ACC (Zhang et al., 2004), but several segments of the protein are not included in the atomic model due to disorder (Zhang et al., 2003, 2004). Residues 2048–2080 (helices α6B and α6C of the C domain), and about 10 residues at the N terminus, are disordered in all three monomers (Figure 1D). Near the C terminus, fragmented electron density was observed based on the crystallographic analysis, but it could not be confidently interpreted in terms of the amino acid sequence of the protein. As a result, about 40 residues are absent from the current atomic model at the C terminus. This additional electron density is located in the dimer interface. Deletion mutants missing the C-terminal segment are monomeric in solution and catalytically inactive (unpublished data).

Binding Mode of CP-640186

CP-640186 is bound in the active site of the CT domain, at the interface between the two monomers of the CT dimer (Figure 1D). The compound is present in all three independent active sites in the crystal, in essentially the same conformation. The anthracene group of the inhibitor is held tightly between helix α6 in the N domain and helix α6′ in the C domain (with the prime indicating the second monomer) (Figure 2A). The structure suggests that only a flat chemical moiety can fit in this part of the binding site. The carbonyl oxygen atom next to the anthracene group is hydrogen bonded to the main chain amide of Glu2026′ near the beginning of helix α6′,

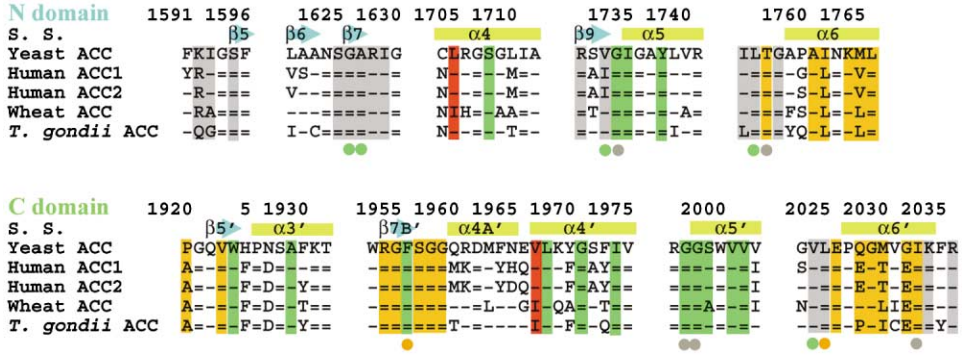

Figure 3. The Inhibitor Binding Sites Are Highly Conserved

Sequence alignment of residues in the CP-640186 (highlighted in gold), haloxyfop (in green), and CoA (in gray) binding pockets. The two residues that confer herbicide resistance when mutated, Leu1705 and Val1967, are highlighted in red (Delye et al., 2003; Zagnitko et al., 2001). A dash represents a residue that is identical to that in yeast ACC, whereas an equal sign represents a residue that is strictly conserved among ACCs.

whereas that next to the morpholine ring is hydrogen bonded to the main chain amide of Gly1958′ (Figure 2B). The geometry of the latter hydrogen bond is not optimal, as the angle between the carbonyl and the amide groups is about 90° (Figure 2A).

The two piperidyl rings and the morpholino group are all in the favored chair conformation (Figure 2A). They are placed in a deep, mostly hydrophobic groove on the surface of the active site (Figure 2C). One wall of this groove is formed by the side chains of Pro1920′, Val1923′, Arg1954′, and Glu2026′ (Figure 2B), while the other is formed by Thr1757, Ile1762, Met1765, and Leu1766 from the α6 helix of the N domain (Figure 2A). With the exception of Ile1762, Met1765, and Pro1920′, the other residues in this binding groove are strictly conserved among the ACCs (Figure 3, and see below).

Our structure suggests that the hydrophobic groove that interacts with the piperidyl and the morpholino groups of CP-640186 may also be the binding site for the biotin substrate in the CT domain (Figure 4A). (Each full-length ACC enzyme actually has three biotin binding sites, one each in the BC, BCCP, and CT domains. The biotin binding site in this paper refers to that in the CT domain.) CP-640186 has no overlap with the bound position of CoA in the active site (Figure 4B) (Zhang et al., 2003), but the piperidyl rings are within 7 Å of the thiol group of CoA and approach the active site from the opposite direction of CoA (Figure 4A). This is the expected location of the biotin substrate of the CT enzyme. It is unlikely for the biotin substrate to approach the active site from the direction of the CoA molecule, as there will be steric hindrance between the two substrates. Therefore, the most likely direction for biotin to approach the active site is from the opposite side of the CoA molecule, where the CP-640186 compound is bound (Figure 4A).

Our structural observation is supported by kinetic studies with full-length ACC showing CP-640186 is noncompetitive versus the acetyl-CoA substrate (Harwood et al., 2003), as well as our own kinetic studies with the

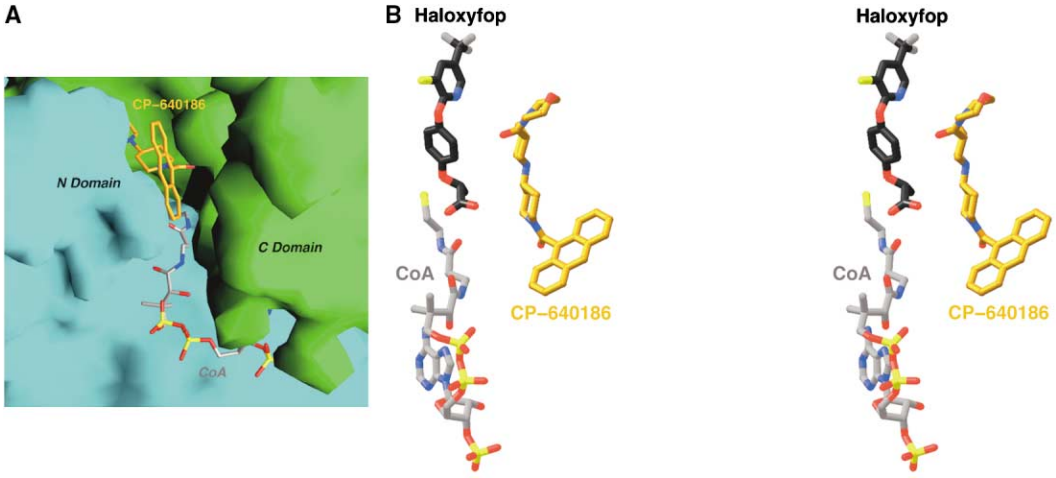

Figure 4. Three Distinct Binding Regions in the Active Site of CT

(A) Molecular surface of the active site region of yeast CT. The CoA and CP-640186 molecules are shown in gray and gold, respectively. This panel was produced with Grasp (Nicholls et al., 1991).

(B) Comparison of the binding modes of CP-640186 (in gold), haloxyfop (black), and CoA (gray). This panel was produced with Ribbons (Carson, 1987).

isolated CT domain (see below). The structural information therefore predicts that CP-640186 should be a competitive inhibitor with respect to the biotin substrate. Our attempts at demonstrating this pattern of inhibition were not successful, due to the high K_m (around 10 mM) of the biotin substrate (Polakis et al., 1974).

The morpholine portion of CP-640186 is important for high-affinity binding to the mammalian ACCs (Harwood et al., 2003). The compound that has only a simple amino group at this position is a much weaker inhibitor, with IC_{50} value of 1.8 μM (Harwood et al., 2003). Our structure shows that the morpholine ring is situated in the hydrophobic groove (Figure 2C), consistent with its importance for binding affinity. At the same time, there appears to be additional space near this group in the binding site (Figure 2C). This is supported by the observation that compounds that replace the morpholine ring with bulkier groups, such as diisopropylamine, are more potent than CP-640186 (Harwood et al., 2003).

The structure of the complex also explains the molecular basis for the stereoselectivity of the binding (Harwood et al., 2003). The *R* stereoisomer of CP-640186 allows interactions between the morpholino group and the CT domain, while this group in the *S* stereoisomer would be projected out of the binding site, possibly also having steric clashes with the enzyme (Figure 2C). Indeed, the *R* and *S* stereoisomers of the closely related diethylamide derivative (CP-610431 and CP-610432, respectively [Harwood et al., 2003]) inhibit rat liver ACC1 with IC_{50} values of 36 and 5000 nM, respectively (H.J. Harwood, personal communication).

There are only minor conformational changes in the CT domain upon inhibitor binding. The overall structure of the CT domain, as well as the organization of the dimer, in the CP-640186 complex is essentially the same as that of the free enzyme that we reported earlier (Zhang et al., 2003, 2004).

Distinct Mechanisms for Inhibiting the CT Domain

Both CP-640186 and the herbicides are potent inhibitors of their target ACCs (Devine and Shukla, 2000; Gronwald, 1991; Harwood et al., 2003), and our structural studies demonstrate that both compounds function at the active site of the CT domain (Figure 1D) (Zhang et al., 2004). However, CP-640186 and the FOPs have distinct mechanisms for inhibiting the CT activity, as they have no overlap in their bound positions (Figure 4B). While CP-640186 may utilize the putative biotin binding site of the CT domain, the FOPs are bound in an allosteric site that is unlikely to be occupied by either substrate of the enzyme during catalysis (Zhang et al., 2004).

Moreover, herbicide binding requires changes in the conformation of several residues in the dimer interface, as well as in the organization of the dimer (Zhang et al., 2004). This is in sharp contrast to our observations on the complex with CP-640186, where the compound is associated with a preformed binding site.

As a consequence of these conformational changes, CP-640186 and the FOPs should be competitive with each other for binding to the CT domain, although this is an indirect competition, as the two compounds do not have any overlap in the CT active site (Figure 4B). The conformation of Phe1956′ in the herbicide complex is incompatible with CP-640186 binding. This residue is located in strand β7B′ of the C domain, whose main chain is in direct contact with the CP-640186 inhibitor (Figure 2A). Our binding studies confirm this prediction based on the structural information (see below).

Inhibition of Yeast CT Domain by CP-640186

To assess whether isolated CT domains can maintain similar affinity for the inhibitors as the full-length ACC enzymes, we carried out kinetic and fluorescence binding studies to characterize the inhibition of the yeast CT domain by CP-640186. Kinetic studies show that the compound has an IC_{50} value of about 8 μM (Figure 5A). It is a noncompetitive inhibitor with respect to the substrate malonyl-CoA (Figure 5B), with inhibitory constants of 4.9 and 6.0 μM for K_{ii} and K_{is}, respectively. This pattern of inhibition is consistent with results from kinetic studies on the full-length ACCs (Harwood et al., 2003) as well as our structural observation.

The inhibitory potency against the isolated CT domain from yeast ACC is essentially the same as that against full-length ACCs from other fungal sources (IC_{50} values for the closely related diethylamide derivative, CP-610431, of 6 μM against *Candida* ACC and 1 μM against *Aspergillus* ACC) (Harwood et al., 2003). This demonstrates that the other domains of fungal ACCs may only have a minor role in the binding of CP-640186, and suggests that the isolated CT domains, in addition to the full-length ACCs, can serve as a direct drug discovery target.

The presence of the anthracene fluorophore in CP-640186 allowed us to develop a fluorescence anisotropy assay that directly measures the binding affinity between the inhibitor and the CT domain. The observed titration curve (fluorescence anisotropy versus CT domain concentration) can be readily fit to a 1:1 binding model (Figure 5C), giving a K_d value of 7.2 μM, essentially the same as the kinetic observations. This confirms that there is only one binding site for CP-640186 in each CT domain.

As our structural data suggest that CP-640186 and the FOPs herbicides should be competitive in their binding to the CT domain, we next performed a competition binding assay. The decrease in fluorescence anisotropy of CP-640186 in the presence of haloxyfop confirmed the competitive nature of the binding (Figure 5D). The affinity of haloxyfop for the CT domain can be deduced from the observed data, and the resulting K_d value of 200 μM is in good agreement with the K_i value of 250 μM that we determined from kinetic studies earlier (Zhang et al., 2003).

Inhibition of Human CT Domain by CP-640186 and CP-640188

We have produced small amounts of the CT domain of human ACC1 by expression in bacteria, and kinetic studies confirm that this CT domain is catalytically active (data not shown). The fluorescence anisotropy binding assay developed using the yeast CT domain allowed us to characterize the inhibition of the human CT by CP-

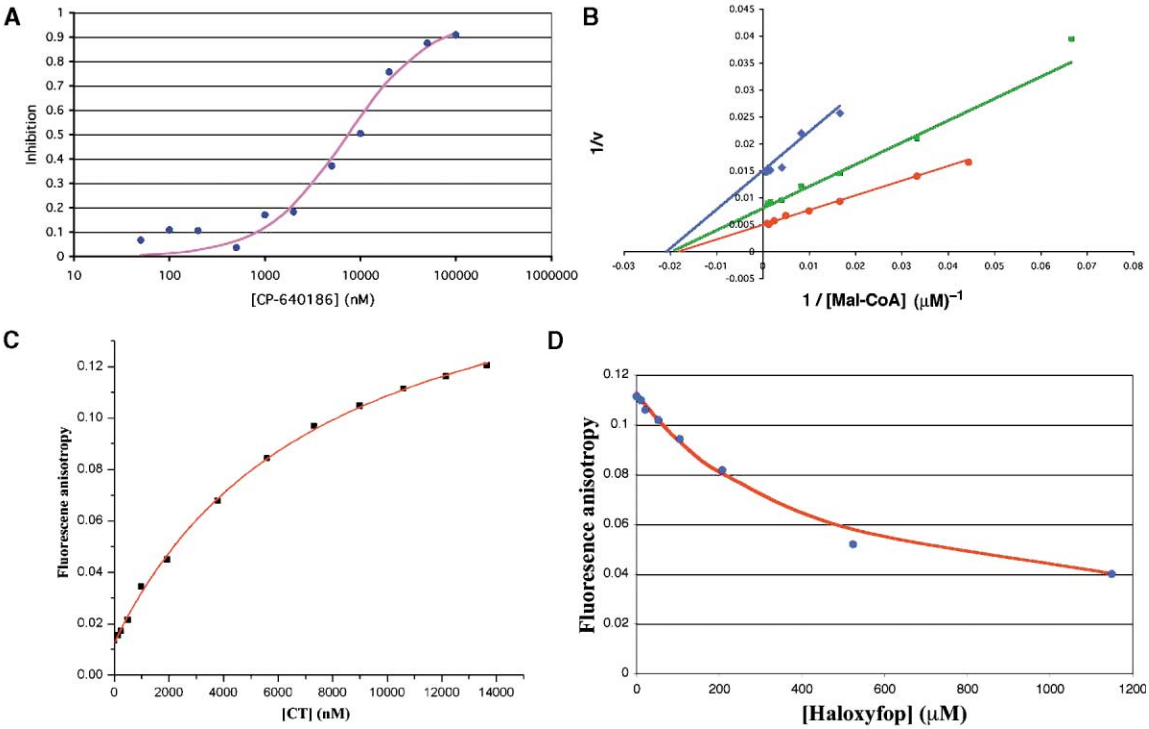

Figure 5. The Inhibition of Yeast CT Domain

The data from one representative experiment of several duplicates are shown.

(A) Titration curve for the determination of the IC_{50} value of CP-640186 against the yeast CT domain.

(B) Double reciprocal plot showing the noncompetitive inhibition of the yeast CT domain by CP-640186. Red, 0 μM; green, 3 μM; and blue, 10 μM CP-640186.

(C) Plot of the fluorescence anisotropy of CP-640186 as a function of yeast CT domain concentration. The observed binding curve can be fit to a 1:1 binding model.

(D) The fluorescence anisotropy of CP-640186 as a function of the concentration of the haloxyfop competitor.

640186 and its more potent analog, CP-640188, which contains the diisopropylamide moiety in place of the morpholine ring (Harwood et al., 2003). The K_d values for the isolated CT domains as determined from the binding assays are 1.2 and 0.5 μM for CP-641086 and CP-640188, respectively (Figure 6).

The observed K_d values for the CT domain are 20–50 fold higher than the IC_{50} values of these compounds against full-length rat ACCs (55 and 10 nM, respectively) (Harwood et al., 2003). One possible explanation for this difference is that other domains of mammalian ACCs, especially BCCP, might play a role in the binding of CP-640186. Part of the morpholine ring is exposed to the solvent in the complex (Figure 2C). It may be possible that the BCCP domain, which carries the biotin substrate in the full-length enzyme, helps shield this ring from the solvent and thereby enhances the binding affinity of CP-640186 to the mammalian ACCs. Our data with the yeast CT domain suggest the other domains of fungal ACCs may have only a minor role in binding CP-640186, but there are biochemical differences between the mammalian and fungal ACCs. For example, the mammalian enzyme is activated by citrate (Wakil et al., 1983), and the IC_{50} values for CP-640186 were measured in the presence of this activator (Harwood et al., 2003). It would be interesting to determine whether citrate has an impact on the IC_{50} value of the compound.

Conservation of the Binding Site

The CT domains of yeast and human ACCs share 50% amino acid sequence identity overall. In the active site region, the degree of sequence conservation is even higher (Figure 3). It may be expected that the binding mode of CP-640186 to the mammalian CT domains should be the same as that to the yeast CT domain reported here. Most of the residues that directly contact the CP-640186 inhibitor are strictly conserved among the ACCs (Figure 3). In fact, all the residues in the binding site for CP-640186 are identical between human ACC1 and ACC2 (Figure 3), consistent with the potent activity of this compound against both isoforms of mammalian ACCs (Harwood et al., 2003).

Ile1762, Met1765, and Pro1920 near the piperidyl and morpholino groups, and Gln2028, Met2030, and Gly2032 near the anthracene group, are the only residues that show differences between the yeast and human ACCs in this binding site (Figure 3). To assess the impact of these variations on the affinity for CP-640186, we created three single-site mutants, I1762L, M1765V, and G2032E, of the yeast CT domain, which introduced the equivalent residue from human ACCs. These three residues were chosen because it appears they make stronger contacts with CP-640186 (Figure 2A). Our kinetic and binding data show that the I1762L and G2032E mutations have only minor effects on the catalytic activ-

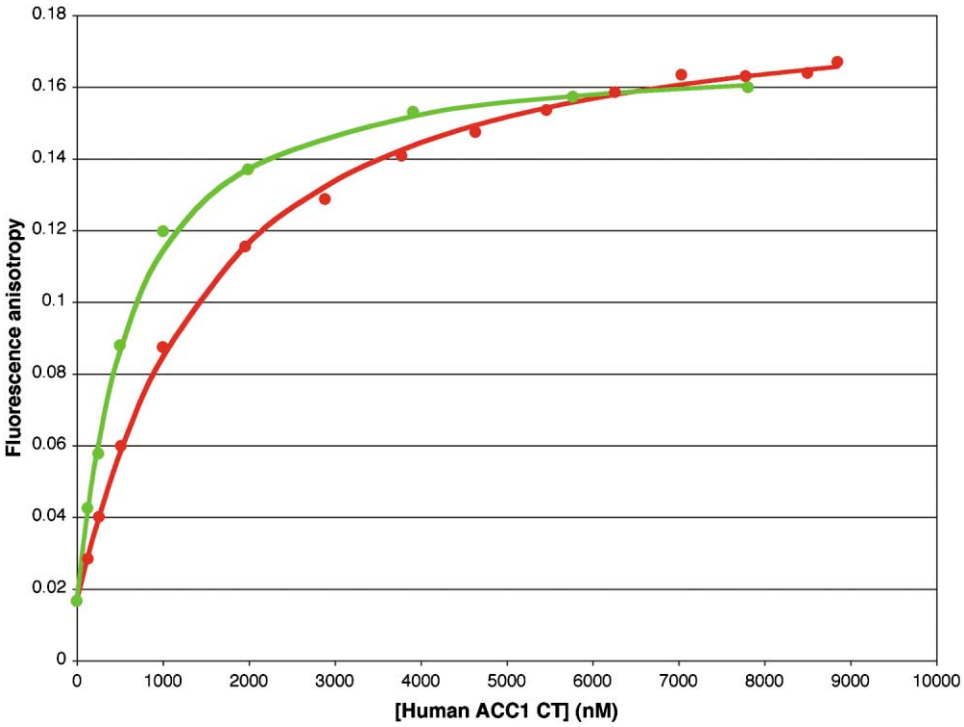

Figure 6. The Inhibition of the CT Domain of Human ACC1

Plot of the fluorescence anisotropy of CP-640186 (red) or CP-640188 (green) as a function of CT domain concentration.

ity of the CT domain and the affinity for CP-640186 (data not shown). The M1765V mutant did not produce enough soluble enzyme for kinetic or binding studies. It remains to be seen whether a mutant carrying all the changes at the same time can have higher affinity for the compound.

It is possible that the specificity of mammalian ACCs for CP-640186 is determined by residues outside the immediate binding site. We have observed a similar situation for the herbicides, where mutation of residues that directly contact haloxyfop is not sufficient to make the yeast CT domain sensitive to the compound (Zhang et al., 2004). In addition, as discussed above, other domains of mammalian ACCs, for example BCCP, may also play a role in the binding of CP-640186, providing another mechanism for the potent inhibition of the mammalian ACCs by these compounds.

Three Distinct Regions for Drug Discovery in the Active Site of CT

Our structural studies of the substrate and inhibitor complexes of the CT domain reveal that the active site of this enzyme has three distinct regions for binding small molecules—the CoA binding region, the putative biotin binding region, and the herbicide binding region (Figure 4B). There is little overlap among the three regions, and the relevance of these regions for drug discovery is illustrated by the fact that inhibitors with nanomolar potency have already been developed utilizing the biotin and the herbicide binding regions. It is likely that potent inhibitors can also be developed against the CoA binding region. It is also conceivable that compounds that bridge the different regions could also be potent inhibitors of the CT activity.

While the CoA and the putative biotin regions correspond to substrate binding sites, the herbicide binding region is an allosteric binding surface and requires large conformational changes for two strictly conserved residues near the active site of the enzyme, Tyr1738 and Phe1956′ (Zhang et al., 2004). Conformational changes in the active site have been observed in other drug discovery targets, for example in the binding of Gleevec to the Abelson tyrosine kinase (Schindler et al., 2000) and the binding of potent inhibitors to p38 MAP kinase (Pargellis et al., 2002).

Although both CP-640186 and the herbicides were originally identified based on their inhibition of full-length ACCs, the large size of these enzymes (Figure 1A) essentially precludes any detailed structural studies of the interactions between the inhibitors and the full-length enzymes. Therefore, the characterization of inhibitor binding to the CT domain may represent the only means of elucidating the molecular basis of their actions. Our structural and kinetic studies demonstrate that these compounds have intimate associations with the CT domain and potently inhibit its activity. This suggests that the CT domain itself may also be a valid target for the development of inhibitors against the ACCs. The three binding regions in this domain identified from our studies should allow the design and development of new, potent inhibitors against these important therapeutic targets.

Experimental Procedures

Protein Production and Crystallization

The cloning, expression, purification, and crystallization of the CT domain (residues 1476–2233) of yeast ACC followed protocols as

described earlier (Zhang et al., 2003, 2004). The free enzyme was crystallized with the hanging-drop vapor diffusion method. The reservoir solution contains 0.1 M sodium citrate (pH 5.5), 200 mM NaCl, 8% (w/v) PEG8000, and 10% (v/v) glycerol. The protein is at 10 mg/ml concentration.

The CT domain (residues 1548–2346) of human ACC1 was subcloned into the pET24d vector (Novagen) and expressed in *E. coli*. The soluble enzyme was purified by nickel-affinity and anion-exchange chromatography. From 6 liters of bacterial culture, the typical yield of purified human CT domain is about 2 mg.

To prepare the CP-640186 complex, crystals of the free enzyme of yeast CT were soaked with 1 mM concentration of the compound for 24 hr and then flash-frozen in liquid propane for data collection at 100 K.

Structure Determination

X-ray diffraction data were collected at the X4A beamline of the National Synchrotron Light Source (NSLS). The diffraction images were processed with the HKL package (Otwinowski and Minor, 1997). The crystal belongs to space group *C*2, with unit cell parameters of a = 246.8 Å, b = 125.2 Å, c = 145.5 Å, and $\beta = 94.1^\circ$. The structure refinement was carried out with the program CNS (Brunger et al., 1998). The atomic model was modified with the program O (Jones, 1978). The inhibitor was included in the refinement after the protein residues had been rebuilt to fit the electron density. The R value for the model with only protein atoms was 24.4% (R_{free} of 28.1%).

Mutagenesis and Kinetic Assays

The mutants of the yeast CT domain were created with the QuikChange kit (Stratagene). They were sequenced, expressed in *E. coli,* and purified following the same protocol as that for the wild-type CT domain.

The catalytic activity of the CT domain was assayed following protocols described earlier, monitoring the production of NADH that is coupled to the formation of acetyl-CoA from malonyl-CoA (Guchhait et al., 1974; Zhang et al., 2003). The kinetic parameters were extracted from the velocity data by nonlinear least squares fitting (Cleland, 1979).

Fluorescence Anisotropy Binding Assay

These experiments were performed on a Photon Technology International fluorimeter. Increasing concentrations of the yeast CT domain were titrated into a solution that initially contained 100 mM Tris (pH 8.0), 100 mM NaCl, and 1 μM CP-640186. The excitation wavelength was 350 nm, and the fluorescence emission was monitored between 390 and 430 nm. The observed fluorescence anisotropy of the compound as a function of the CT domain concentration is fitted to a 1:1 binding model to extract the binding constant K_d. The experiments were repeated several times, using different concentrations of CP-640186, which gave essentially the same results for the K_d. For the binding assay with the human CT domain, the concentration of CP-640186 and CP-640188 was 0.5 and 0.2 μM, respectively.

For the competitive binding assay, increasing concentrations of haloxyfop were titrated into a solution that initially contained 100 mM Tris (pH 8.0), 100 mM NaCl, 0.5 μM CP-640186, and 8 μM yeast CT domain. The final concentration of haloxyfop was limited to about 1.2 mM due to poor solubility.

Acknowledgments

We thank James Harwood and David Perry of Pfizer Global Research and Development for providing the CP-640186 and CP-640188 compounds and helpful discussions; Randy Abramowitz and Xiaochun Yang for setting up the beamline at X4A; W.W. Cleland for providing the software for analyzing kinetic data; Yang Shen and Xiao Tao for help with data collection at the synchrotron source; and Nathan Karpowich for help with the fluorescence experiment. This research is supported in part by a grant from the NIH (DK67238) to L.T.

Received: May 18, 2004
Revised: July 1, 2004
Accepted: July 2, 2004
Published: September 7, 2004

References

Abu-Elheiga, L., Matzuk, M.M., Abo-Hashema, K.A.H., and Wakil, S.J. (2001). Continuous fatty acid oxidation and reduced fat storage in mice lacking acetyl-CoA carboxylase 2. Science *291*, 2613–2616.

Abu-Elheiga, L., Oh, W., Kordari, P., and Wakil, S.J. (2003). Acetyl-CoA carboxylase 2 mutant mice are protected against obesity and diabetes induced by high-fat/high-carbohydrate diets. Proc. Natl. Acad. Sci. USA *100*, 10207–10212.

Alberts, A.W., and Vagelos, P.R. (1972). Acyl-CoA carboxylases. In The Enzymes, P.D. Boyer, ed. (New York, Academic Press), pp. 37–82.

Brunger, A.T., Adams, P.D., Clore, G.M., DeLano, W.L., Gros, P., Grosse-Kunstleve, R.W., Jiang, J.-S., Kuszewski, J., Nilges, M., Pannu, N.S., et al. (1998). Crystallography & NMR system: a new software suite for macromolecular structure determination. Acta Crystallogr. D Biol. Crystallogr. *54*, 905–921.

Carson, M. (1987). Ribbon models of macromolecules. J. Mol. Graph. *5*, 103–106.

Cleland, W.W. (1979). Statistical analysis of enzyme kinetic data. Methods Enzymol. *63*, 103–138.

Cronan, J.E., Jr., and Waldrop, G.L. (2002). Multi-subunit acetyl-CoA carboxylases. Prog. Lipid Res. *41*, 407–435.

Delye, C., Zhang, X.-Q., Chalopin, C., Michel, S., and Powles, S.B. (2003). An isoleucine residue within the carboxyl-transferase domain of multidomain acetyl-coenzyme A carboxylase is a major determinant of sensitivity to aryloxyphenoxypropionate but not to cyclohexanedione inhibitors. Plant Physiol. *132*, 1716–1723.

Devine, M.D., and Shukla, A. (2000). Altered target sites as a mechanism of herbicide resistance. Crop Prot. *19*, 881–889.

Evans, S.V. (1993). SETOR: hardware lighted three-dimensional solid model representations of macromolecules. J. Mol. Graph. *11*, 134–138.

Gronwald, J.W. (1991). Lipid biosynthesis inhibitors. Weed Sci. *39*, 435–449.

Guchhait, R.B., Polakis, S.E., Dimroth, P., Stoll, E., Moss, J., and Lane, M.D. (1974). Acetyl coenzyme A carboxylase system from Escherichia coli. Purification and properties of the biotin carboxylase, carboxyltransferase, and carboxyl carrier protein components. J. Biol. Chem. *249*, 6633–6645.

Harwood, H.J., Jr., Petras, S.F., Shelly, L.D., Zaccaro, L.M., Perry, D.A., Makowski, M.R., Hargrove, D.M., Martin, K.A., Tracey, W.R., Chapman, J.G., et al. (2003). Isozyme-nonselective N-substituted bipiperidylcarboxamide acetyl-CoA carboxylase inhibitors reduce tissue malonyl-CoA concentrations, inhibit fatty acid synthesis, and increase fatty acid oxidation in cultured cells and in experimental animals. J. Biol. Chem. *278*, 37099–37111.

Hill, J.O., Wyatt, H.R., Reed, G.W., and Peters, J.C. (2003). Obesity and the environment: where do we go from here? Science *299*, 853–855.

Jelenska, J., Sirikhachornkit, A., Haselkorn, R., and Gornicki, P. (2002). The carboxyltransferase activity of the apicoplast acetyl-CoA carboxylase of Toxoplasma gondii is the target of aryloxyphenoxypropionate inhibitors. J. Biol. Chem. *277*, 23208–23215.

Jones, T.A. (1978). A graphics model building and refinement system for macromolecules. J. Appl. Crystallogr. *11*, 268–272.

Lenhard, J.M., and Gottschalk, W.K. (2002). Preclinical developments in type 2 diabetes. Adv. Drug Deliv. Rev. *54*, 1199–1212.

McGarry, J.D., and Brown, N.F. (1997). The mitochondrial carnitine palmitoyltransferase system. From concept to molecular analysis. Eur. J. Biochem. *244*, 1–14.

Nicholls, A., Sharp, K.A., and Honig, B. (1991). Protein folding and association: insights from the interfacial and thermodynamic properties of hydrocarbons. Proteins *11*, 281–296.

Otwinowski, Z., and Minor, W. (1997). Processing of X-ray diffraction data collected in oscillation mode. Methods Enzymol. *276*, 307–326.

Pargellis, C., Tong, L., Churchill, L., Cirillo, P.F., Gilmore, T., Graham, A.G., Grob, P.M., Hickey, E.R., Moss, N., Pav, S., et al. (2002). Inhibi-

tion of p38 MAP kinase by utilizing a novel allosteric binding site. Nat. Struct. Biol. *9*, 268–272.

Polakis, S.E., Guchhait, R.B., Zwergel, E.E., and Lane, M.D. (1974). Acetyl coenzyme A carboxylase system of Escherichia coli. Studies on the mechanisms of the biotin carboxylase- and carboxyltransferase-catalyzed reactions. J. Biol. Chem. *249*, 6657–6667.

Ramsay, R.R., Gandour, R.D., and van der Leij, F.R. (2001). Molecular enzymology of carnitine transfer and transport. Biochim. Biophys. Acta *1546*, 21–43.

Rendina, A.R., Craig-Kennard, A.C., Beaudoin, J.D., and Breen, M.K. (1990). Inhibition of acetyl-coenzyme A carboxylase by two classes of grass-selective herbicides. J. Agric. Food Chem. *38*, 1282–1287.

Schindler, T., Bornmann, W., Pellicena, P., Miller, W.T., Clarkson, B., and Kuriyan, J. (2000). Structural mechanism for STI-571 inhibition of Abelson tyrosine kinase. Science *289*, 1938–1942.

Wakil, S.J., Stoops, J.K., and Joshi, V.C. (1983). Fatty acid synthesis and its regulation. Annu. Rev. Biochem. *52*, 537–579.

Zagnitko, O., Jelenska, J., Tevzadze, G., Haselkorn, R., and Gornicki, P. (2001). An isoleucine/leucine residue in the carboxyltransferase domain of acetyl-CoA carboxylase is critical for interaction with aryloxyphenoxypropionate and cyclohexanedione inhibitors. Proc. Natl. Acad. Sci. USA *98*, 6617–6622.

Zhang, H., Tweel, B., and Tong, L. (2004). Molecular basis for the inhibition of the carboxyltransferase domain of acetyl-coenzyme A carboxylase by haloxyfop and diclofop. Proc. Natl. Acad. Sci. USA *101*, 5910–5915.

Zhang, H., Yang, Z., Shen, Y., and Tong, L. (2003). Crystal structure of the carboxyltransferase domain of acetyl-coenzyme A carboxylase. Science *299*, 2064–2067.

Accession Numbers

The PDB entry code reported in our paper is 1W2X.